Quantitative Elastic-Property Measurements at the Nanoscale with Atomic Force Acoustic Microscopy**

By *D. C. Hurley,** *M. Kopycinska-Müller*, *A. B. Kos*, and *R. H. Geiss*

We are developing metrology for rapid, quantitative assessment of elastic properties with nanoscale spatial resolution. Atomic force acoustic microscopy (AFAM) methods enable measurements of modulus at either a single point or as a map of local property variations. The information obtained furthers our understanding of nanopatterned surfaces, thin films, and nanoscale structures.

1. Introduction

New measurement tools are required in the rapidly burgeoning field of nanotechnology. In particular, information about mechanical properties on the nanoscale is needed. Knowledge of mechanical properties such as elastic modulus, strain, and adhesion is critical to successful development of new films and nanoscale assemblies. Such information is also needed to assess integrity or reliability in applications from microelectronics to biotechnology. The demand for nanomechanical information is fuelled by the fact that applications often involve multiple materials integrated on the micro- or nanoscale (*e.g.*, electronic interconnects, composites). The complexity of fabricating such systems dictates the use of predictive modeling in order to reap savings in cost and time. Modeling can correctly predict system performance only if the property data used as input are accurate at the relevant length scales. Furthermore, in such heterogeneous systems it is frequently the localized variation or divergence in properties that causes failure (void formation, fracture, etc.). Thus it is increasingly important to assess not the "average" sample properties, but to obtain quantitative images of the spatial distribution in properties.

Many conventional methods for mechanical-property measurements have drawbacks: they are destructive, not quantitative, limited to specialized geometries, and so on. Nanoindentation[1] is currently one of the most commonly used tools for this purpose. However, existing nanoindentation techniques face serious measurement challenges as dimensions shrink further and applications increasingly use very compliant ("soft") materials. In such systems, the volume sampled by nanoindentation may be too large for adequate spatial resolution due to the indenter tip's relatively large radius and the relatively large loads applied. A promising method combines low-load nanoindentation techniques with force modulation and scanning.[2] However, the lateral resolution is still limited by the radius of the Berkovich diamond indenter used (a few hundred nanometers).

An alternative approach for nanomechanical property measurements exploits the spatial resolution of the atomic force microscope (AFM). The small diameter of the AFM tip (~10–100 nm), the low applied loads (~0.1–5 μN), and the scanning capability of the AFM promise *in-situ* elastic-property imaging with nanoscale spatial resolution. Accordingly, several types of AFM-based methods to measure nanomechanical properties have been demonstrated. Methods that show the most promise of quantitative information are dynamic

[*] *D. C. Hurley, M. Kopycinska-Müller, A. B. Kos, R. H. Geiss*
National Institute of Standards & Technology
325 Broadway, Boulder, Colorado 80305-3328, USA
E-mail: hurley@boulder.nist.gov

[**] *We value the contributions to this work made by J. Müller, P. Rice, and J. Wright (NIST). We thank J. Turner (Univ. Nebraska-Lincoln, USA) and W. Arnold, S. Hirsekorn, U. Rabe (IZFP, Germany) for valuable discussions. The nanoindentation measurements were provided by N. Jennett (NPL, UK), A. Rar (Univ. Tennessee-Knoxville, USA), and D. Smith (NIST). We are grateful to G. Pharr (Univ. Tennessee-Knoxville, USA), Y. Dzenis (Univ. Nebraska-Lincoln, USA), P. Dresselhaus, G. Hilton, W. Rippard, and S. Russek (NIST) for providing samples.*

 DOI: 10.1002/adem.200500039 © 2005 WILEY-VCH Verlag GmbH & Co. KGaA, Weinheim

approaches in which the AFM cantilever is vibrated at or near its resonant frequencies.[3] Several of these techniques are labelled "acoustic" or "ultrasonic" methods, based on the characteristic frequency range (~0.1–3 MHz) of the cantilever used. Among these methods are ultrasonic force microscopy,[4] heterodyne force microscopy,[5] ultrasonic atomic force microscopy,[6] and atomic force acoustic microscopy (AFAM).[7]

Of these methods, AFAM has arguably achieved the most progress in *quantitative* measurement of elastic properties. However, further refinement is needed to improve AFAM's accuracy and range of applicability. In our research, we seek to understand which aspects of the measurement process most strongly influence repeatability, accuracy, and related issues. Here, we describe our progress towards quantitative measurements of nanoscale elastic properties with AFAM. We first summarize the basic experimental and theoretical concepts of AFAM. Next, we demonstrate the validity of the basic measurement method with results for several thin films. Studies to investigate the effects of film thickness, and work to extend AFAM methods to achieve rapid contact-stiffness imaging are also discussed. Through this work, we hope to contribute to the understanding of nanomechanical properties and their measurement.

2. The AFAM Method

In simplest terms, AFAM involves exciting and measuring the resonant frequencies of the AFM cantilever beam when the cantilever tip is in contact with a sample (the "contact-resonance frequencies"). The resonant frequencies are analyzed with a model for cantilever dynamics to determine the contact stiffness that characterizes the interaction between the tip and the sample. From the contact stiffness, the elastic properties of the sample are calculated from a suitable model for the tip-sample contact. Here we summarize the basic experimental and theoretical concepts involved. More detailed descriptions have been published previously.[8,9]

Figure 1(a) shows a block diagram of the experimental apparatus used to measure the elastic modulus at a fixed position. The sample of interest is mounted on a commercial ultrasonic contact transducer with a piezoelectric element. The transducer is excited with a continuous sine wave voltage by a function generator (frequency ~0.1–3.5 MHz, amplitude ~25–500 mV). When the tip of the AFM cantilever is brought in contact with the sample at an applied load F_c, the frequencies of the resonant modes increase from their free-space values due to tip-sample forces that stiffen the system. Here we consider only the two lowest flexural (bending) modes of the cantilever. To detect the amplitude of the cantilever vibration, the AFM photodiode signal is processed by a lock-in amplifier. In this way, a spectrum of the cantilever response versus frequency can be obtained by sweeping the transducer excitation frequency and recording the lock-in output signal.

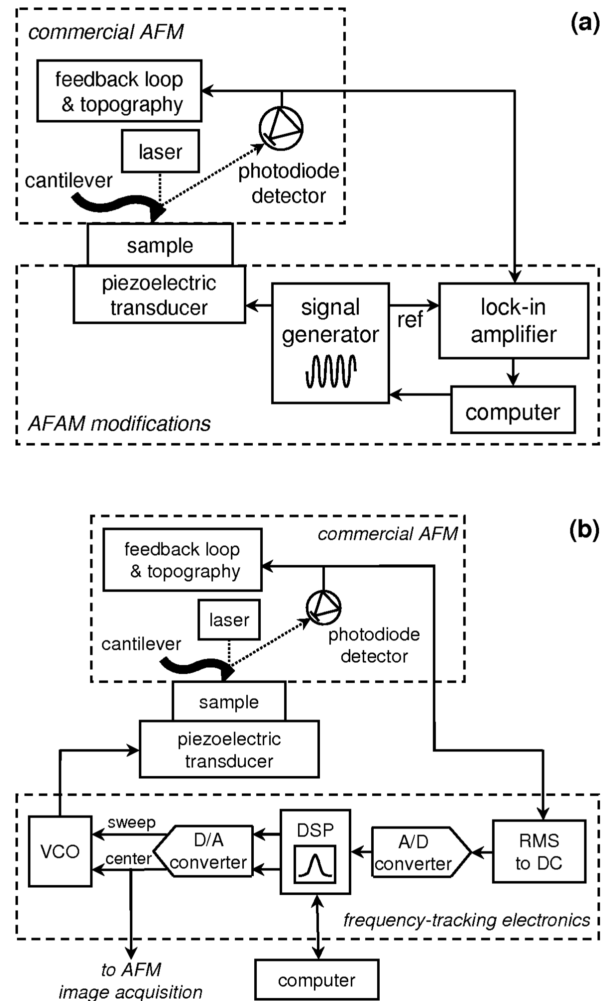

Fig. 1. Schematic of experimental AFAM apparatus used for (a) modulus measurements at a fixed sample position and (b) contact-resonance-frequency imaging.

The experimental frequency spectra are interpreted with an analytical or finite-element model for the cantilever beam dynamics.[8] The beam-dynamics model relates the measured frequencies to one or more parameters that characterize the tip-sample interaction. The simplest model to describe the interaction is a spring of stiffness k^* between the tip and the sample representing a purely elastic interaction. This approximation is valid if the applied load F_c is much greater than the adhesive force but low enough to avoid plastic deformation of the sample. Such conditions apply under typical experimental conditions involving relatively stiff materials (*e.g.*, metals, ceramics) and stiff cantilevers (spring constant $k_c \approx$ 40–50 N/m) for which $F_c \approx$ 0.4–2 μN.

From the values of k^*, the elastic properties of the sample can be calculated from an appropriate model of the tip-sample contact mechanics.[10] Most commonly used are Hertzian contact mechanics, which describe the elastic interaction

 © 2005 WILEY-VCH Verlag GmbH & Co. KGaA, Weinheim

between a hemispherical tip of radius R pressed against a flat surface with an applied force F_c. In this case, k^* can be calculated from

$$k^* = \sqrt[3]{6F_C R E^{*2}} \quad (1)$$

Here E^* is the reduced Young's modulus, defined by

$$\frac{1}{E^*} = \frac{1}{M_t} + \frac{1}{M_s} \quad (2)$$

M_s and M_t correspond to the indentation moduli of the sample and the AFM tip. For elastically isotropic materials $M = E/(1\text{-}\nu^2)$, where E is Young's modulus and ν is Poisson's ratio. In anisotropic materials, M depends on direction and is calculated from the second-order elastic stiffness tensor.[11] For the <100> silicon AFM tip, we use M_t = 165 GPa.

It is difficult in practice to determine the values for R needed in Eq. 1. Therefore, the AFAM method uses a reference material with known elastic properties to compare values of k^*:[12]

$$E_s^* = E_{ref}^* \left(\frac{k_s^*}{k_{ref}^*} \right)^n \quad (3)$$

The subscript *ref* refers to the reference sample and n depends on the tip-sample geometry. For Hertzian contact, $n = 3/2$; for a "flat punch" (flat tip), $n = 1$. M_s for the sample can therefore be calculated from Eqs. 2 and 3 without direct knowledge of R. Usually, several measurements are made on the reference material before and after measurements on the sample of interest. All of the results are averaged to obtain a single value for M_s in order to minimize the effects of tip wear.

3. Quantitative Modulus Measurements with AFAM

3.1. Comparison with Nanoindentation

In order to verify AFAM methods for quantitative elastic-property measurements, we have performed experiments on several thin-film samples. Blanket films of a variety of materials (as shown in Fig. 2) were sputtered on single-crystal silicon wafer substrates. For each sample, we compared values for the indentation modulus M obtained from AFAM to those measured by nanoindentation. The nanoindentation experiments were performed by several different laboratories (see Acknowledgments). Different sections of the same sample were used for the AFAM and nanoindentation measurements. The film thickness t was determined by analysis of the sample in cross section in a scanning electron microscope (SEM) or with a stylus profilometer.

Figure 2 shows the results of our comparison between AFAM and nanoindentation measurements of M. It can be seen that the films possessed a fairly wide range of stiffness

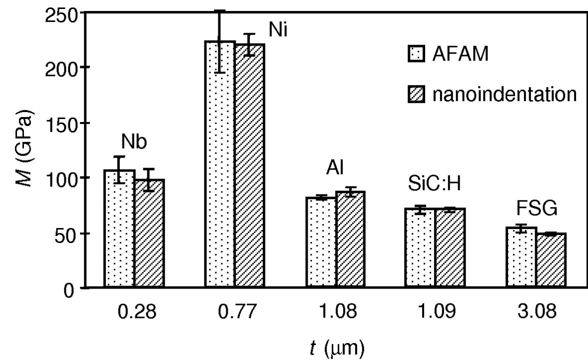

Fig. 2. Comparison between AFAM and nanoindentation results. The chart shows the measured values of the indentation modulus M for several supported thin films: niobium (Nb), nickel (Ni), aluminum (Al), hydrogenated silicon carbide (SiC:H), and fluorinated silica glass (FSG). The thickness t of each film is also shown. The error bars represent the standard deviation in the multiple measurements due to scatter.

(~50–250 GPa) and thickness (~0.3–3 μm) values. The figure shows that the AFAM and nanoindentation results are in very good agreement (differences of less than 10 % and within the measurement uncertainty) for all of the samples. Furthermore, the absolute values for M fall within the range of bulk literature values for all but one material. (The exception is the nickel film, which is discussed below and in Ref. 13.) These results give us confidence in our quantitative AFAM methods.

3.2. Effects of Film Thickness on Measurement Accuracy

Interpretation of nanoindentation measurements on thin-film samples is often hindered by the fact that the mechanical properties of the substrate affect the measured values. The critical thickness at which these effects become significant, and therefore at which more complex measurement procedures are required, depends on the properties of both the film and substrate. In general, a film thickness of about 1 μm is used as rule of thumb. AFAM measurements of thin-film samples may also contain substrate effects, but the critical thickness should be much lower due to the smaller contact radius and applied forces. To investigate this issue, we performed AFAM experiments on a series of thin-film samples. The films were sputter-deposited nickel on (001) silicon substrates with nominal thicknesses of 800 nm, 200 nm, and 50 nm. SEM and x-ray diffraction (XRD) analysis indicated that the films were nanocrystalline with a strong (111) fiber texture.

Table 1 shows our results for the nickel-film samples. Literature values for the indentation modulus M of single-crystal nickel range from approximately 220 GPa in the <100> direction to 250 GPa in the <111> direction. Therefore, the values of M measured by AFAM were lower than expected for <111>-textured nickel. Because the (001) silicon substrate is more compliant than the nickel film (M = 165 GPa), substrate effects might be the reason for the reduced values of M. To determine whether this was the case, the values of stress and

 © 2005 WILEY-VCH Verlag GmbH & Co. KGaA, Weinheim

Table 1. Results for nanocrystalline nickel thin-film samples. The film thickness t and average grain diameter d were determined by SEM analysis. M_{AFAM} is the indentation modulus measured by AFAM. The uncertainties represent the standard deviation due to scatter in individual measurements.

t (nm)	*d* (nm)	M_{AFAM} (GPa)
772 ± 5	23 ± 8	223 ± 28
204 ± 4	20 ± 6	220 ± 19
53 ± 2	11 ± 3	210 ± 26

deformation at the sample surface and at the film-substrate interface were estimated. If the stress and deformation in the substrate at the film-substrate interface are negligible compared to their values directly under the tip, then substrate effects can be safely ignored. For the film approximately 800 nm thick, the substrate deformation at the film-substrate interface was about 0.1 % of its value at the tip, and the stress at the interface was less than 0.03 % of its value directly under the tip. For the thinnest film, which was approximately 50 nm thick, the estimated stress amplitude at the interface ranged from 3 to 6 % of its value under the tip, depending on experimental conditions. The corresponding deformation in the substrate at the film-substrate interface was about 4 to 8 % of its value under the tip. We consider these values of stress and deformation to be negligible.

From these results we conclude that AFAM can directly measure the modulus of very thin films ($t < 100$ nm), without the need to account for substrate effects. The film thickness for which the substrate begins to play a role depends on the elastic properties of both the tip and sample. Although such conclusions have significant implications for AFAM measurements, it means that thickness effects probably did not cause the observed reduction in *M*. We believe that a more likely explanation is the nanocrystalline nature of the nickel films. Nanocrystalline films contain an increased volume fraction of intercrystalline material with reduced modulus. Calculations of *M* with nanocrystalline models that include intercrystalline material and the measured grain diameters agree with the measured AFAM values of *M*. A detailed discussion is available elsewhere.[13]

3.3. Quantitative AFAM Imaging

Although these results demonstrate the validity of quantitative AFAM measurements at a *fixed position*, we ultimately desire quantitative *imaging* of elastic properties. To achieve this objective, we must track the contact-resonance frequencies as the tip moves across the sample. However, simply combining fixed-position AFAM techniques with two-dimensional scanning is impractical because it could take days to acquire a single image.[6] Our solution differs from those described previously[6,7] in that it is based on digital signal processor (DSP) methods. A schematic of the frequency-tracking apparatus is shown in Figure 1(b). A swept-frequency sinusoidal voltage is applied to the piezoelectric transducer. The photodiode signal amplitude is processed by a root-mean-square-to-DC (RMS-to-DC) converter (bandwidth ~1 kHz to 3.2 MHz) and sent to an analog-to-digital (A/D) converter. From the RMS voltage response as the frequency is swept, the circuit constructs a complete resonance curve and finds its peak. A digital feedback control loop uses this information to adjust a voltage-controlled oscillator (VCO) that tunes the center frequency of vibration. In this way, the sweep window remains centered on the cantilever resonance. The control voltage is also sent to the AFM's auxiliary image input port. Each image pixel therefore contains a value proportional to the peak (*i.e.*, contact-resonance) frequency at that position. With the specific circuit components used, a scan rate of 0.2 Hz (5 s/line) is usually sufficient for scans several micrometers in size. Thus a 256 × 256 image takes approximately 22 min to acquire.

Figures 3 and 4 show images obtained with the frequency-tracking electronics described above. The images in Figure 3 correspond to a composite sample with glass fibers embedded in a polymer matrix. Figure 3(a) shows the sample topography (height) and was acquired at the same time as one of the frequency images. Figures 3(b) and (c) are images of the first (f_1) and second (f_2) flexural modes, respectively. Figure 3(d) contains the normalized contact stiffness k^*/k_c obtained from the images of f_1 and f_2. It was calculated on a pixel-by-pixel basis with the single-point AFAM methods described above. Figure 3(d) indicates that the contact stiffness (and thus presumably the modulus) are generally higher for the (glass) fibers than the (polymer) matrix. This is qualitatively consistent with typical values for the relative moduli of glass and polymer. More importantly, this image reveals that the stiffness

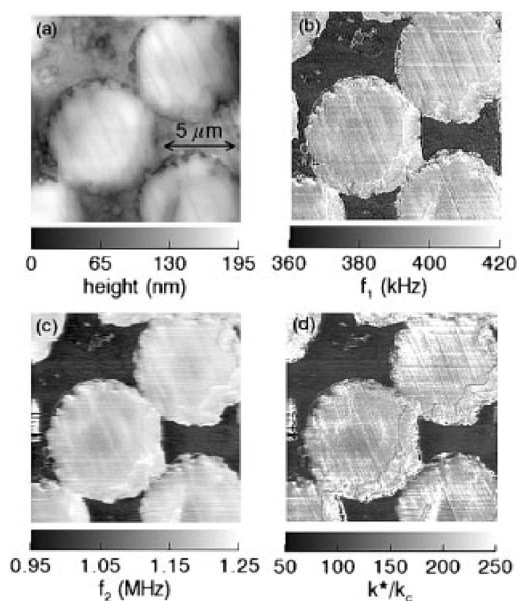

Fig. 3. Examples of quantitative AFAM images. (a) Topography of a glass-fiber/polymer matrix composite. Images of (b) the first flexural mode f_1 and (c) the second flexural mode f_2. (d) Normalized vertical contact stiffness k^*/k_c calculated from (b) and (c).

 © 2005 WILEY-VCH Verlag GmbH & Co. KGaA, Weinheim

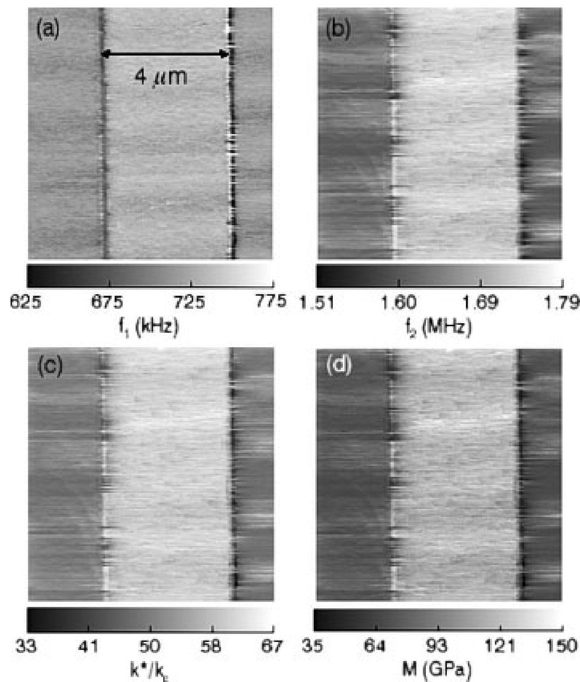

Fig. 4. Quantitative AFAM images for a Nb/SiO_2 thin-film sample. Contact-resonance frequency images of (a) f_1 and (b) f_2. (c) Normalized contact stiffness k^*/k_c calculated from (a) and (b). (d) Indentation modulus M calculated from (c) assuming Hertzian contact mechanics.

in the center of each fiber is slightly lower than the surrounding region. This information cannot be obtained from topography images such as that in Figure 3(a).

Contact-stiffness images aid in visualizing relative property distributions, but maps of the elastic modulus are the ultimate goal. Figure 4 shows how contact-resonance frequency images can be used to obtain a modulus map. The sample was a silicon wafer on which a silica (SiO_2) blanket film (thickness ~350 nm) had been deposited by plasma-assisted chemical vapor deposition. On top of the SiO_2 film was a niobium (Nb) stripe (~200 nm thick × 4 μm wide). Contact-resonance frequency images for the Nb/SiO_2 sample are shown in Figures 4(a) and (b). The central Nb stripe has greater values for f_1 and f_2 compared to the left and right SiO_2 film regions. This is consistent with quantitative fixed-point AFAM experiments on the films that yielded M_{SiO2} = 75.1 ± 10.0 GPa for the SiO_2 film and M_{Nb} = 112.7 ± 15.0 GPa for the Nb film. The measured values fall within the range of literature values for bulk fused silica (M_{SiO2} ≈ 72–77 GPa) and bulk Nb (M_{Nb} ≈ 116–133 GPa). The very narrow, bright and dark vertical lines indicate relatively large, spurious frequency changes due to the rapid change in height (~180 nm) between the SiO_2 and Nb films.

An image of the normalized contact stiffness k^*/k_c calculated from the images of f_1 and f_2 is given in Figure 4(c). To obtain an image of the indentation modulus M, we used Hertzian contact mechanics and assumed that the mean value of k^*/k_c for the SiO_2 region corresponded to the previously measured value of M_{SiO2} = 75.1 GPa. In the resulting image shown in Figure 4(d), the mean value for M in the entire SiO_2 region is M_{SiO2} = 75.5 ± 7.1 GPa, while the mean value for the Nb film region is M_{Nb} = 118.5 ± 7.1 GPa. This is in good agreement with both the fixed-point value and the bulk literature values mentioned above.

4. Summary and Conclusions

AFAM is a contact AFM method involving dynamic modes of the cantilever. It provides quantitative elastic-property values with nanoscale spatial resolution. AFAM values for the indentation modulus M measured at a fixed sample position are in good agreement with results obtained by more established techniques such as nanoindentation. AFAM has successfully measured M for films as thin as 50 nm, which present serious challenges for current nanoindentation approaches. To achieve nanoscale elastic-property mapping, we have developed DSP-based tools that combine quantitative AFAM methods with two-dimensional scanning. The resulting images of contact-resonance frequencies will enable us to map the contact stiffness and elastic properties of surfaces and nanoscale structures.

Although these and other results from groups worldwide show significant promise, true quantitative nanomechanical imaging requires further effort. To improve measurement accuracy and repeatability, we must better understand and control issues such as surface topography, tip wear, and the actual tip-sample contact behavior. For example, current AFAM methods involve scanning the silicon AFM tip across a material of roughly equivalent stiffness, so that tip damage or wear is inevitable. Changes in the tip radius affect the contact-resonance frequencies and hence the measured values of M. Other challenges arise for AFAM measurements of very soft materials, for which adhesive forces cannot be ignored. Resolving such issues is likely to result in refinements to the AFAM technique, enhancing its value as a quantitative measurement tool and leading to increased information about material properties on the nanoscale.

Received: March 02, 2005
Final version: March 16, 2005

[1] W. C. Oliver, G. M. Pharr, *J. Mater. Res.* **1992**, *7*, 1564.
[2] S. A. Syed Asif, K. J. Wahl, R. J. Colton, O. L. Warren, *J. Appl. Phys.* **2001**, *90*, 1192.
[3] Q. Zhong, D. Inniss, K. Kjoller, V. B. Elings, *Surface Science* **1993**, *290*, L688.
[4] R. E. Geer, O. V. Kolosov, G. A. D. Briggs, G. S. Shekhawat, *J. Appl. Phys.* **2002**, *91*, 4549.
[5] M. T. Cuberes, H. E. Assender, G. A. D. Briggs, O. V. Kolosov, *J. Phys. D: Appl. Phys.* **2000**, *33*, 2347.
[6] K. Yamanaka, Y. Maruyama, T. Tsuji, K. Nakamoto, *Appl. Phys. Lett.* **2001**, *78*, 1939.

 © 2005 WILEY-VCH Verlag GmbH & Co. KGaA, Weinheim

RESEARCH NEWS

[7] U. Rabe, M. Kopycinska, S. Hirsekorn, J. Muñoz Saldaña, G. A. Schneider, W. Arnold, *J. Phys. D: Appl. Phys.* **2002**, *35*, 2621.
[8] U. Rabe, S. Amelio, E. Kester, V. Scherer, S. Hirsekorn, W. Arnold, *Ultrasonics* **2000**, *38*, 430.
[9] D. C. Hurley, K. Shen, N. M. Jennett, J. A. Turner, *J. Appl. Phys.* **2003**, *94*, 2347.
[10] K. L. Johnson, *Contact Mechanics*, Cambridge University Press, Cambridge **1985**, Ch. 4-5.
[11] J. J. Vlassak, W. D. Nix, *Phil. Mag. A* **1993**, *67*, 1045.
[12] U. Rabe, S. Amelio, M. Kopycinska, S. Hirsekorn, M. Kempf, M. Göken, W. Arnold, *Surf. Interf. Anal.* **2002**, *33*, 65.
[13] M. Kopycinska-Müller, R. H. Geiss, J. Müller, D. C. Hurley, *Nanotechnology* **2005**, *16*, 703.

 © 2005 WILEY-VCH Verlag GmbH & Co. KGaA, Weinheim